J. Biochem. **141,** 421–428 (2007)
doi:10.1093/jb/mvm046

Cloning and Characterization of Ferredoxin and Ferredoxin-NADP$^+$ Reductase from Human Malaria Parasite

Yoko Kimata-Ariga[1,*], Genji Kurisu[1,†], Masami Kusunoki[1], Sayaka Aoki[2], Dan Sato[2], Tamaki Kobayashi[3], Kiyoshi Kita[3], Toshihiro Horii[2] and Toshiharu Hase[1]

[1]Institute for Protein Research, Osaka University, 3-2 Yamadaoka, Suita; [2]Department of Molecular Protozoology, Research Institute for Microbial Diseases, Osaka University, Suita, Osaka 565-0871, Japan; and [3]Department of Biomedical Chemistry, Graduate School of Medicine, The University of Tokyo, 7-3-1 Hongo, Bunkyo-ku, Tokyo 113-0033, Japan

Received December 1, 2006; accepted January 17, 2007; published online January 23, 2007

The human malaria parasite (*Plasmodium falciparum*) possesses a plastid-derived organelle called the apicoplast, which is believed to employ metabolisms crucial for the parasite's survival. We cloned and studied the biochemical properties of plant-type ferredoxin (Fd) and Fd-NADP$^+$ reductase (FNR), a redox system that potentially supplies reducing power to Fd-dependent metabolic pathways in malaria parasite apicoplasts. The recombinant *P. falciparum* Fd and FNR proteins were produced by synthetic genes with altered codon usages preferred in *Escherichia coli*. The redox potential of the Fd was shown to be considerably more positive than those of leaf-type and root-type Fds from plants, which is favourable for a presumed direction of electron flow from catabolically generated NADPH to Fd in the apicoplast. The backbone structure of *P. falciparum* Fd, as solved by X-ray crystallography, closely resembles those of Fds from plants, and the surface-charge distribution shows several acidic regions in common with plant Fds and some basic regions unique to this Fd. *P. falciparum* FNR was able to transfer electrons selectively to *P. falciparum* Fd in a reconstituted system of NADPH-dependent cytochrome *c* reduction. These results indicate that an NADPH–FNR–Fd cascade is operative in the apicoplast of human malaria parasites.

Key words: ferredoxin, ferredoxin-NADP$^+$ reductase, human malaria parasite, redox potential, X-ray crystallography.

Abbreviations: cyt *c*, cytochrome *c*; Fd, ferredoxin; FNR, ferredoxin-NADP$^+$ reductase; PfFd, *P. falciparum* Fd; PfFNR, *P. falciparum* FNR

Note: The atomic coordinates for *P. falciparum* Fd have been deposited in the Protein Data Bank www.pdb.org (accession code: 1IUE)

Protozoan parasites of the phylum Apicomplexa, including *Plasmodium sp.* (the causative agent of malaria) and *Toxoplasma sp.*, contain a non-photosynthetic plastid organelle called the apicoplast (*1*). The apicoplast is considered to have been acquired by secondary endosymbiosis of algae (*2*), and is essential for the parasite's survival (*3*, *4*). The vital function of the apicoplast remains unclear, but it is thought to employ metabolisms common to those performed in the plastid of non-photosynthetic tissues, such as roots, in higher plants (*5*). Biosynthesis of fatty acids, isoprenoids, Fe–S clusters and hemes are proposed as such candidates (*6*). Because the apicoplast is non-photosynthetic, energy and reducing power as well as substrates (particularly carbon) for anabolic biosynthesis need to be delivered from outside of the organella. Triose phosphates such as phosphoenolpyruvate and dihydroxyacetone phosphate are suggested to be imported from the cytosol as a carbon source by analogy to non-photosynthetic plastid in plants (*6*). However, the mechanism by which the apicoplast satisfies its energy requirements remains unclear without the discovery of the components for the glycolytic pathway, pentose phosphate pathway, nor ATP/ADP antiporter. One possibility is supply of NAD(P)H through an electron shuttle created by dihydroxyacetone phosphate.

Recently, genes encoding proteins homologous to plant ferredoxin (Fd) and Fd-NADP$^+$ reductase (FNR) were found in the genomes of *Plasmodium falciparum* (human malaria parasite) (*5*) and *Toxoplasma gondii* (*7*). They are both single-copy genes and contain putative N-terminal apicoplast-targeting signals. FNR, an FAD-containing enzyme, is responsible for the electron transfer between NADPH and Fd, a small 2Fe–2S protein. Fd in photosynthetic plastids (chloroplasts) receives electrons from photosystem I, and a large portion of this reduced Fd is utilized by FNR for the conversion of NADP$^+$ to NADPH, needed in the Calvin cycle (*8*). In non-photosynthetic plastids, on the other

*To whom correspondence should be addressed. Tel: +81-6-6879-8611, Fax: +81-6-6879-8613,
E-mail: a-yoko@protein.osaka-u.ac.jp
†Present address: Graduate School of Arts and Sciences, The University of Tokyo, Komaba, Meguro-ku, Tokyo 153-8802, Japan

hand, FNR catalyses the reverse direction of electron transfer from NADPH to Fd, which then acts as a major reductant for various reactions in this organelle such as reduction of nitrite (*9*) and sulphite, and biosynthesis of unsaturated fatty acids.

Fd and FNR are each present as distinct isoproteins in photosynthetic and non-photosynthetic plant tissues, and the electron transfer cascade of NADPH–FNR–Fd in the direction opposite to that occurring in the photosynthetic process is facilitated by a combination of non-photosynthetic isoproteins of Fd and FNR (*10*, *11*). By analogy, a redox cascade of NADPH–FNR–Fd in the apicoplasts is predicted to provide reducing power, which drives putative, possibly crucial, Fd-dependent metabolisms (*5*). The involvement of apicoplast Fd is indicated by the recent discovery of an Fe–S cluster assembly pathway (*12*), fatty acid desaturase (*5*) and isoprenoid biosynthesis pathway (*13*). Because this plant-type redox system is not present in the mammalian host, it would represent a promising drug target to combat malaria, for instance, by developing substances that inhibit the interaction between Fd and FNR.

In order to obtain detailed information about the biochemical properties of Fd and FNR in human malaria parasites (*P. falciparum*), we recombinantly expressed, purified and functionally characterized these proteins.

EXPERIMENTAL PROCEDURES

Preparation of Recombinant Proteins—DNA sequences encoding *P. falciparum* Fd (PfFd) and FNR (PfFNR) were identified by a TBLASTN screen with previously reported amino-acid sequences from maize (*Zea mays* L.) root and *T. gondii* (*5*, *7*) against the Malaria *Plasmodium* database (Plasmo DB) (available at http://plasmodb.org/) in combination with a BLAST search of the malaria genome in the NCBI database. The deduced amino-acid sequences of putative mature PfFd and PfFNR (Plasmo DB accession code PFF1115w) starting from Leu97 and Leu38 of Fd and FNR precursor proteins, respectively, based on the mature sequences of plant Fds and FNRs, were back-translated into the codon usage of *Escherichia coli* because it was considered that the original AT-rich *P. falciparum* sequences would not be efficiently expressed in *E. coli* (*14*, *15*). First Leu of both proteins was replaced by Ala for the purpose of efficient expression in *E. coli*. The A/T ratio of 60 bp from the 5′ end was raised to increase expression level in *E. coli* (*16*). The complete synthetic genes were obtained according to the procedure described previously (*11*) and cloned into the pTrc99A vector (Amersham bioscience). The nucleotide sequences of the chemically synthesized genes for PfFd and PfFNR are shown in supplemental data (supplementary Fig. 1). PfFd protein was expressed and purified from bacteria (JM105) harbouring the above construct, according to the methods described previously (*16*). PfFNR protein was expressed and purified from bacteria (TG1) basically according to the previously described protocol (*10*) except that IPTG concentration was lowered to 20 μM and that Fd-affinity chromatography using PfFd-immobilized Sepharose was applied. At the final step of purification, Phenyl–Superose column (Pharmacia) chromatography was performed with a linear gradient of ammonium sulphate (3-0 M) in 50 mM Tris–HCl (pH 7.5).

Physical Analysis—Spectra were measured on a UV-2500PC spectrophotometer (Shimazu, Tokyo). Redox potential was calculated as the midpoint of cyclic voltammetric measurements made at 25°C versus a Ag/AgCl electrode at pH 7.5 essentially as described by Taniguchi *et al.* (*17*).

Crystallization and Structure Determination—Crystals of PfFd were obtained at 4°C from equal volumes of the concentrated protein (20 mg/ml in 50 mM Tris–HCl, pH 7.5) and reservoir solution [30% (w/v) PEG8000, 200 mM sodium acetate trihydrate and 100 mM sodium cacodylate, pH 6.5] by the hanging-drop vapour diffusion method. X-ray intensity data were collected with a R-AXIS IV imaging plate system (Rigaku) using CuKa radiation. Crystal data and refinement statistics are given in Table 1. Diffraction data were collected with the program d*TREK (*18*). The structure was determined by molecular replacement method using the maize root Fd (FdIII) structure (shown in Fig. 3) as a search model with the program CNS (*19*). Two Fd molecules in the asymmetric unit were refined using the program CNS.

Western Blot and Indirect Immunofluorescence Assay—*P. falciparum* cells (strain Honduras-1) at trophozoite and schizont stages were prepared as previously described (*20*). The parasite cells were disrupted by repeated freezing and thawing, and sonication, and passed through the magnetic purification system of vario MACS column (Miltenyi Biotec) for removal of hemozoin. The resulting cell extract was applied to a DE-52 ion-exchange column for the partial purification of PfFd and used for western blot analysis. Proteins were separated by SDS–PAGE and transferred to PVDF membrane (Immobilon, Millipore) followed by immunodetection essentially according to the methods

Table 1. **Crystallographic data.**

Space group	$P2_1$
a (Å)	49.0
b (Å)	50.6
c (Å)	52.5
b (°)	115.5
Completeness (%)[a]	96.9 (83.5)
R_{merge} (%)[a,b]	8.3 (14.5)
Resolution (Å)	1.7
Number of measured reflections	89,521
Number of unique reflections	24,928
Resolution limits (Å)	47.0–1.7
R_{cryst} (%)[c]	18.4
R_{free} (%)[d]	22.1
Number of water molecules	507
R.M.S. deviations	
Bond lengths (Å)	0.004
Bond angles (°)	1.3

[a]Values for the highest resolution bins (1.76–1.70 Å) are shown in parentheses.
[b]$R_{merge} = \Sigma|I - <I>|/\Sigma I$, where I = observed intensity and $<I>$ = average intensity.
[c]$R_{cryst} = \Sigma|F(obs) - F(calc)|/\Sigma F(obs)$.
[d]R_{free} was calculated against 5% of the total reflections omitted from the refinement.

of Onda *et al*. (*10*). Primary rabbit antibody raised against PfFd was used at 1:1,000 antisera dilution. The antigen–antibody complex was visualized by reaction with alkaline phosphatase conjugated with goat antibodies against rabbit IgG (Bio-Rad).

For subcellular localization of proteins, an indirect immunofluorescence assay was carried out according to the methods described previously (*20*). The antibody was purified using an immobilized PfFd filter, and the antigen–antibody complex was visualized by fluorescence of Cy3 conjugated with sheep antibodies against rabbit IgG (Sigma) for PfFd, and fluorescein isothiocyanate conjugated with sheep antibodies against mouse IgG (Sigma) for iron–sulphur protein subunit of mitochondria complex II (succinate–ubiquinone reductase) from *P. falciparum* (*21*).

Enzymatic Analysis—NADPH-dependent Fd reduction by FNR was measured as described by Onda *et al.* (*10*) except that the concentration of cytochrome *c* (cyt *c*) was lowered to 45 μM and light-path was increased to 1 cm when PfFNR was used.

RESULTS

Physical Properties of PfFd and PfFNR—Recombinant PfFd and PfFNR proteins were produced using synthetic genes (supplementary Fig. 1) with altered codon usages optimized for expression in *E. coli* (*14*, 15). The purified PfFd and PfFNR proteins show typical spectra of 2Fe–2S Fd and flavin-containing enzymes, respectively (Fig. 1), and migrate in SDS–PAGE as homogeneous bands (data not shown).

Redox potential of PfFd was measured together with leaf-type and root-type of Arabidopsis Fds by cyclic voltammetry (Fig. 2). Low redox potential (−310 ~ −450 mV) is characteristic to classical plant-type 2Fe–2S Fds. As shown in Fig. 2, the redox potential of root-type Fd is more positive than that of leaf-type Fd, thus favouring the direction of electron flow from NADPH to Fd in non-photosynthetic tissue while the lower redox potential of leaf-type Fd supports a higher photosynthetic activity, with electron flow in the opposite direction (*11*). The redox potential of PfFd (−266 mV) is even more positive than those of root Fds (Fig. 2A and B). This value is similar to that of mitochondrial adrenodoxin [−250 mV according to ref. (*22*)], another protein containing a 2Fe–2S cluster, which functions as an electron carrier for cytochrome P_{450}s. As the redox potential of the FAD moiety of *T. gondii* FNR is more positive than those of plant

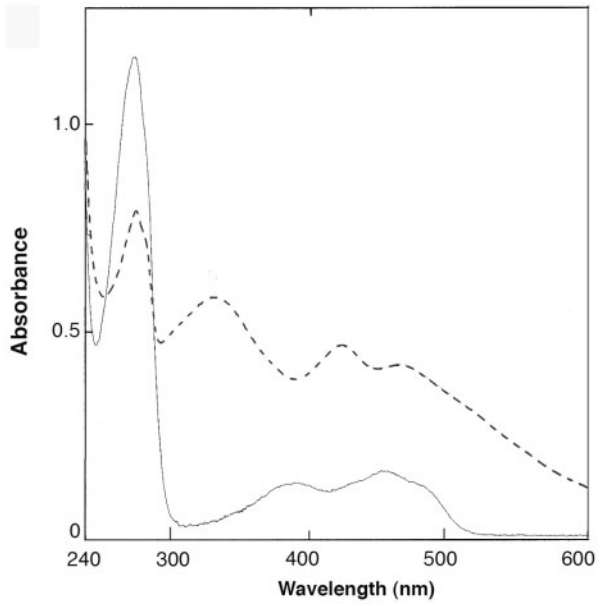

Fig. 1. **Absorption spectra of the recombinant PfFd and PfFNR.** The purified PfFd (210 μM, light path 2 mm) showed the typical spectrum of a 2Fe–2S Fd, with peaks at 277, 332, 424 and 464 nm (dashed line). Maximal absorbance in the UV region was at 277 nm, and a value of 1.75 for the A_{277}/A_{424} ratio was determined as the index of purity. The purified PfFNR (14.8 μM, light path 10 mm) showed the typical spectrum of a flavoprotein, with peaks at 393 and 452 nm (solid line). Maximal absorbance in the UV region was at 275 nm, and a value of 7.0 for the A_{275}/A_{452} ratio was calculated from the spectrum.

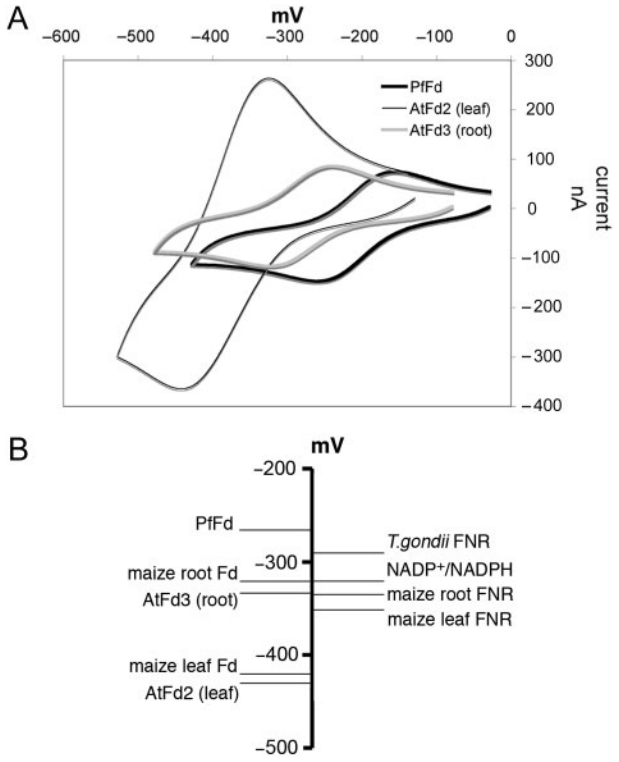

Fig. 2. **Redox potential.** (A) Cyclic voltammograms were taken in 100 μM solutions of *P. falciparum* Fd (PfFd), Arabidopsis leaf-type Fd2 (AtFd2) and Arabidopsis root-type Fd3 (AtFd3), versus a standard hydrogen electrode. Results are typical of at least three independent measurements. SD was <5 mV in all cases. Calculated redox potentials of AtFd2, AtFd3 and PfFd are −433, −337 and −266 mV, respectively. The greater current seen with AtFd2 may be due to its more negative surface charge allowing increased interaction with the electrode, which is coated with positively charged poly–L–Lys, as described in (*11*). (B) Comparison of calculated potentials with known measurements of NADPH and maize and *T. gondii* proteins: maize leaf Fd (*16*); maize root Fd (*29*); leaf FNR and root FNR (*30*); *T. gondii* FNR (*7*).

FNRs [about −290 mV according to ref. (*7*)] (Fig. 2B), the higher redox potential appears to be a characteristic feature of the Fd/FNR couple in apicoplasts.

The amino-acid sequence of the mature region of PfFd shares about 50% homology with plant Fds, but contains several basic residues that are not found in plant Fds (*5*, 7). PfFd was crystallized, and its structure was solved at a 1.7 Å resolution by X-ray diffraction (Fig. 3A, Table 1). The backbone structures of PfFd, maize root Fd and spinach leaf Fd are very similar (except for the C-terminus), with the region surrounding the 2Fe–2S cluster most closely matched (Fig. 3B). While the surface charge distribution around the 2Fe–2S cluster of PfFd is similar to that of plant Fds with most of the surface negatively charged (Fig. 3C upper panels), the opposite surface area of PfFd is more positively charged due to the additional basic residues of Arg at position 8 and Lys at positions 14, 15, 70, 71 and 72 as compared to plant Fds (Fig. 3C lower panels). These basic residues are well conserved among Fds of *Plasmodium sp.* (*P. falciparum*, *P. yoelli* and *P. knowlesi*) and partly conserved with *T. gondii* Fd (Lys14, Lys70 and Lys71), indicative of a parasite-specific character.

Detection and Subcellular Localization of PfFd—Using an antibody against recombinant PfFd, presence of the authentic Fd was confirmed in a DE-52 bound fraction of *P. falciparum* cell extract by western blot (Fig. 4A, lane 4) and its subcellular localization was observed in a discrete area (Fig. 4B, red spots) at the intra-erythrocytic stage of *P. falciparum* cells by indirect immunofluorescence assay. In Fig. 4B, the fluorescent Fd spot was detected in an area adjacent to the nucleus in the early stages (ring and early trophozoite stages in upper panels). This was positioned at an area different from the mitochondria marker signal of succinate–ubiquinone reductase (*21*) (green spot in middle panels). The number of red spots increased later in the trophozoite stage, and they were associated with the divided nuclei at the schizont stage (upper right and lower panels), which agrees with the notion that apicomplexan parasites contain one apicoplast per cell and replication of the organelle precedes cell division (*23*). These observations, together with the presence of its putative N-terminal apicoplast-targeting signal (*7*), strongly indicate that Fd is present in the apicoplast.

Electron Transfer Activity of PfFd and PfFNR—The amino-acid sequence of PfFNR shows unique features, with large insertions and deletions as compared to plant FNRs (*24*). A large insertion of 28 amino acids (with regard to maize root FNR) at position 90 are common to *T. gondii* FNR (*5*, 24), but other insertions and deletions vary between the two apicomplexan FNRs. Experimental evidence that the N-terminal 150-amino-acid (putative apicoplast-targeting) sequence as well as the whole FNR sequence was able to target a genetically fused reporter protein into the apicoplast of *T. gondii* (*25*) supports the localization of FNR in the apicoplast.

Electron transfer activity from PfFNR to PfFd was analysed in a reconstituted system of NADPH-dependent cyt *c* reduction, using leaf-type and root-type Fd and FNR isoproteins from higher plants as controls (Fig. 5).

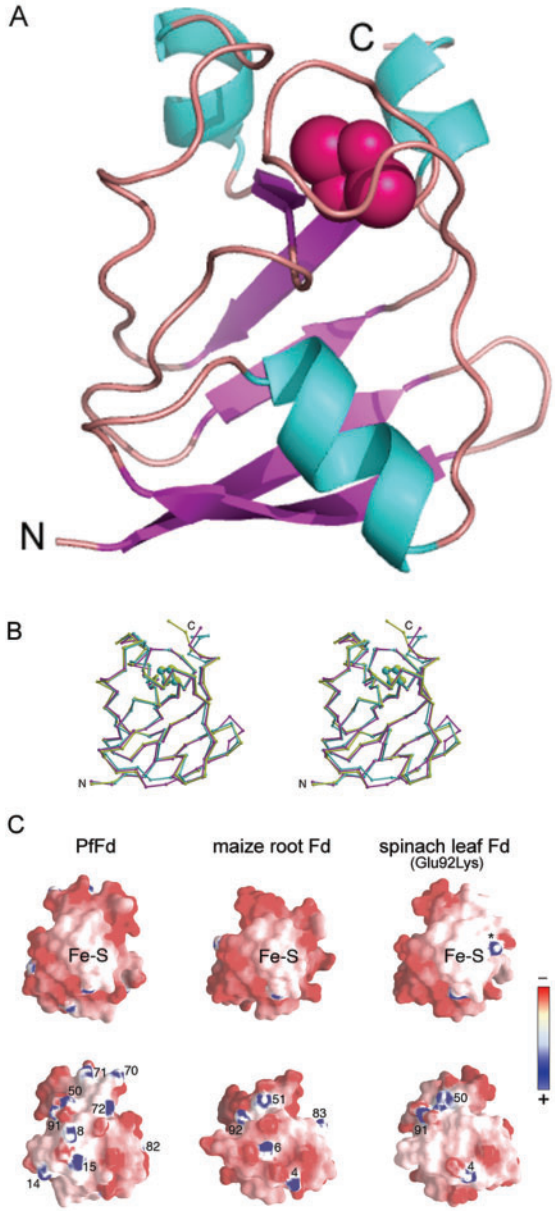

Fig. 3. **Structure of PfFd and comparison with those of higher-plant Fds.** (A) The ribbon diagram of PfFd. The 2Fe–2S cluster is shown as red balls. 'N' and 'C' stand for the N-terminal and C-terminal ends, respectively. (B) Superimposed stereo views of the backbone structures of PfFd (*cyan*), maize (*Zea mays*) root Fd (*magenta*) (PDB, under submission, protein accession number; P27788) and spinach (*Spinacia oleracea*) leaf Fd Glu92Lys mutant (*yellow*) (PDB code 1A70). The 2Fe–2S cluster is shown as a ball-and-stick model. 'N' and 'C' stand for the N-terminal and C-terminal ends, respectively. For spinach leaf Fd, only the crystal structure of a Glu92Lys mutant is available. (C) Surface-charge distribution of PfFd (*Left*), maize root Fd (*Middle*) and spinach leaf Fd Glu92Lys mutant (*Right*), viewed from the side of the 2Fe–2S cluster (*upper*), and from the opposite side of the 2Fe–2S cluster (*lower*). The residue at 92 of spinach leaf Fd [asterisk (*) in upper right panel] is an acidic residue (Glu) in wild-type Fd instead of the basic residue (Lys) in the mutant Fd shown in this figure. In lower panels, the residues with basic charges on the molecular surface are numbered. The figure was produced with GRASP. The bar shown in the right represents the surface-charge gradient from negative (red) to positive (blue).

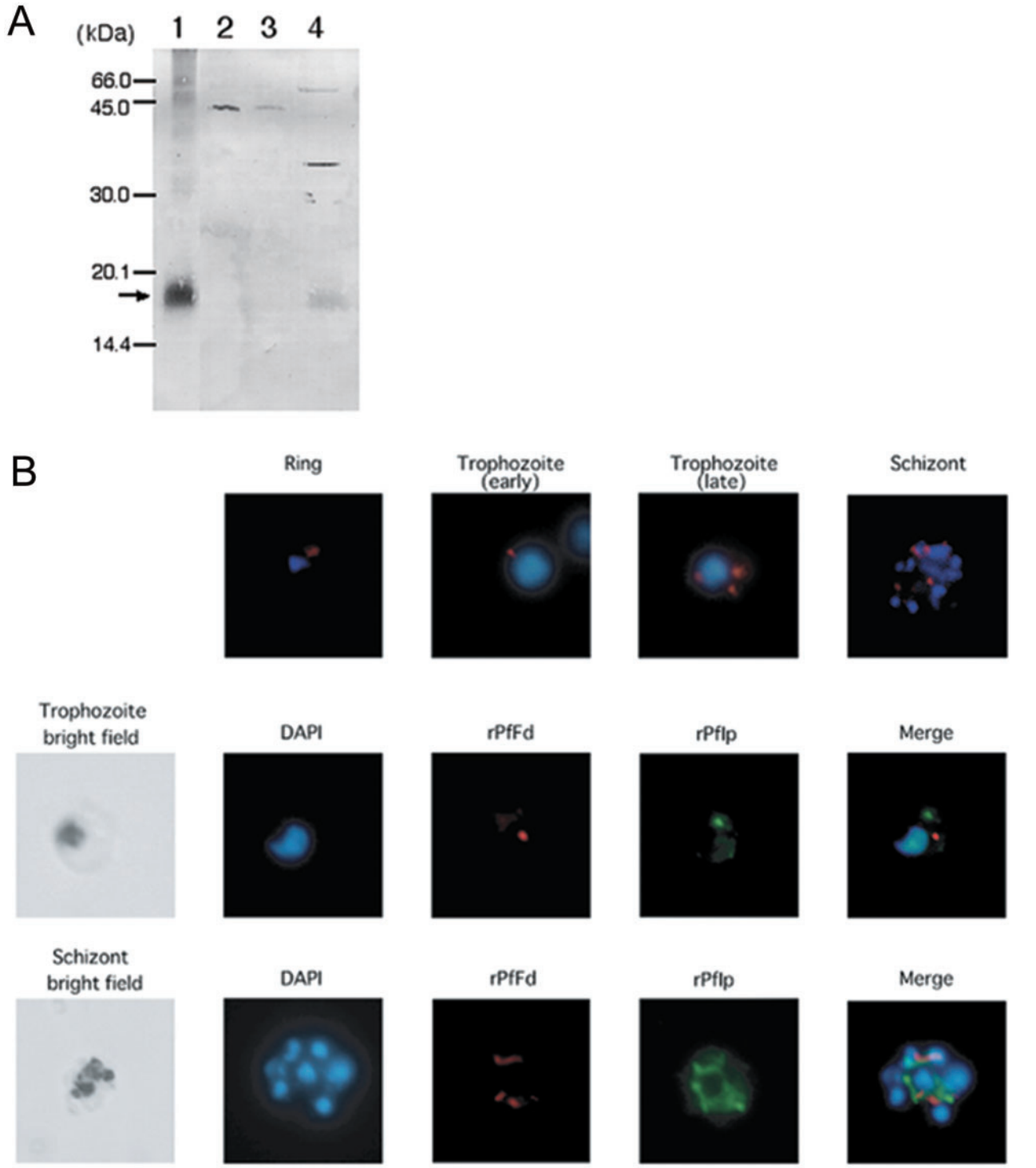

Fig. 4. **Identification and subcellular localization of PfFd in the parasite.** (A) Extract of washed cell cultures of trophozoite and schizont stages of *P. falciparum* (10^8 parasites) was applied to a DE-52 column for the partial purification of Fd, and the resulting unbound fraction (lane 2), washed fraction (lane 3) and eluted fraction (lane 4) were subjected to SDS–PAGE and analysed by western blot together with the purified recombinant PfFd (rPfFd) (10 ng, lane 1) using rabbit antiserum directed against purified rPfFd. The band detected at about 18 kDa (arrow) corresponds to Fd. (B) Ring, early and late trophozoite and schizont stages of *P. falciparum* parasites were subjected to immunofluorescence staining using rabbit antiserum directed against the recombinant PfFd (rPfFd) (*red colour*). Nuclear DNA was counterstained with 4′,6′-diamino-2-phenylindole (DAPI) (*blue colour*). Early trophozoite (*middle panels*) and schizont (*lower panels*) stages of parasites were also subjected to immunofluorescence staining using mouse antiserum directed against the recombinant *P. falciparum* iron–sulphur protein subunit of mitochondria complex II [succinate–ubiquinone reductase, ref. (*21*)] (rPfIp) (*green colour*), as a mitochondrial marker. Colour images of DAPI, rPfFd and rPfIp were obtained independently and overlaid (*merge*). Dark spots in bright field (*left panels*) represent the hemozoin pigment.

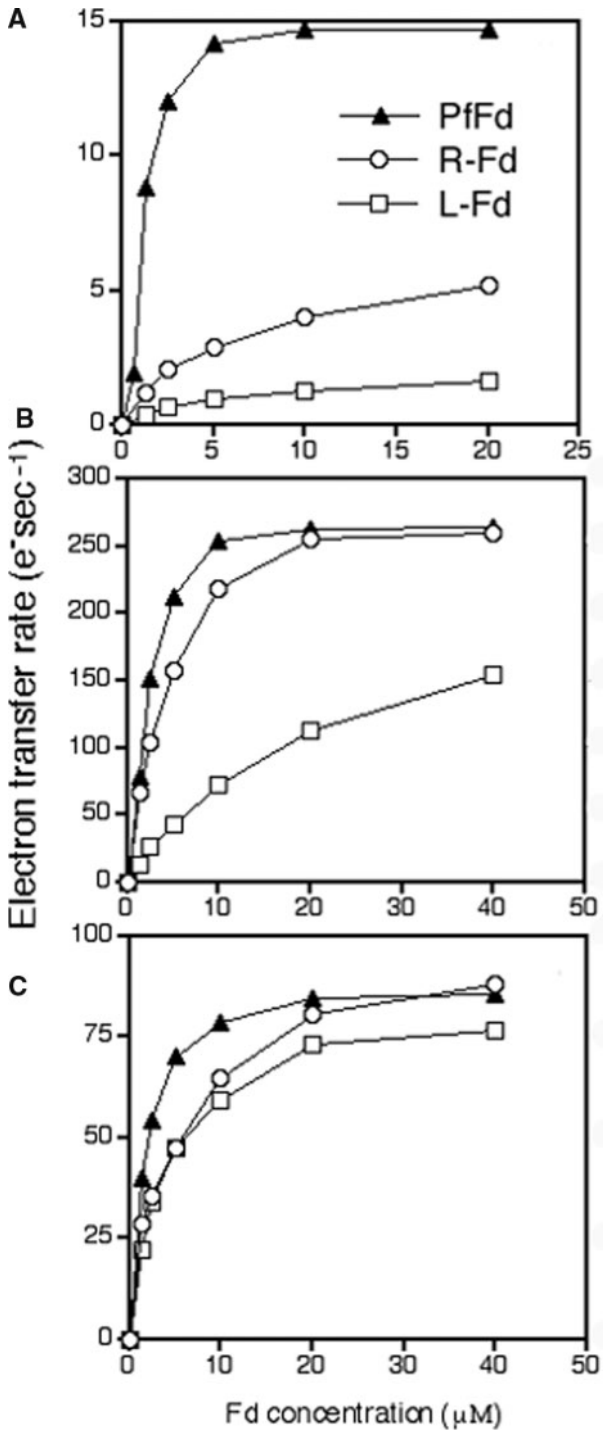

Fig. 5. **Electron transfer activity between Fd and FNR from *P. falciparum* and higher plants.** Electron transfer activity from FNR to Fd was assayed in a reconstituted cascade of NADPH–FNR–Fd–cyt *c* by measuring the rate of cyt *c* reduction. Reactions were performed with combinations of FNR from *P. falciparum* (A), maize root (B) or maize leaf (C) and Fd from *P. falciparum* (PfFd), maize root (R-Fd) or spinach leaf (L-Fd). Recombinant Fd and FNR isoproteins from maize and spinach were purified as reported previously (*10*, *16*). Basically the same results were obtained when maize leaf Fd was used in place of spinach leaf Fd. Typical results of three independent experiments are presented. Note that PfFNR selectively transfers electrons to PfFd (A), maize root FNR transfers electrons more efficiently to PfFd and root Fd than to leaf Fd (B), and in the case of maize leaf FNR, a similar profile is seen with all the three Fds (C). The results of the combinations of leaf and root Fd/FNR (B and C) are consistent with our previous reports (*10*, *11*).

PfFNR transfers electrons to PfFd most effectively among the three Fds tested (Fig. 5A), suggesting an advantageous combination of PfFNR and PfFd. On the other hand, plant FNRs transfer electrons to PfFd at an equal or slightly higher efficiency than to plant Fds. The k_{cat} value of PfFNR was found to be considerably lower than those of plant FNRs (*10*) (Fig. 5) and *T. gondii* FNR (*7*). This is due to inherently lower activity (k_{cat}) of NADPH oxidation as measured by diaphorase activity (about one-fifth of root-type FNR, Kimata-Ariga, Y. and Hase, T., unpublished observations). The rate of NADH oxidation by the FNR was found to be still lower than that with NADPH (Kimata-Ariga, Y. and Hase, T., unpublished observations). These results indicate that an NADPH–FNR–Fd cascade is operative in the apicoplast.

DISCUSSION

In this study, we have structurally and biochemicaly characterized Fd and FNR of *P. falciparum* and provided clear evidence that the functional NADPH/FNR/Fd redox cascade is present in the apicoplast of malaria parasites. The X-ray crystal structure of PfFd showed a remarkable similarity with those of the plant counterparts. The higher redox potential of PfFd is apparently favourable for electron flow from catabolically generated NADPH to Fd in the apicoplast, and electron transfer from PfFNR to PfFd is specific, although the rate is slow relative to higher plant FNR : Fd reactions.

The difference in redox potential between 2Fe–2S cluster proteins is thought to be due to electrostatic interactions between the polypeptide environment and the active site cluster (*26*). However, the primary sequence and 3D structures of leaf, root and apicoplast Fds around the active site region are very similar except for Thr/Ser at position 46 (PfFd nomenclature), which has distinct conservation in root (& apicoplast)/leaf-type Fds and determines a small change in redox potential in cyanobacterium Anabaena Fd (*27*). Our recent study (*28*) using recombinant chimeras of leaf and root Fds suggests that residue changes far from the redox centre have the potential to affect the microenvironment of the 2Fe–2S cluster through long-distance effects, resulting in relatively large changes in the redox potential. It is therefore possible that residues distant from the 2Fe–2S cluster may be the cause of the higher redox potential of PfFd than leaf and root Fds. Apicoplast Fd-specific basic residues such as Lys14 and Lys70-71 (shown in Fig. 3C) may be responsible for the higher redox potential.

The slower electron transfer rate of PfFNR/PfFd is likely to be related to the character of the redox proteins that receive electrons from Fd in the apicoplast. In fact, major Fd-dependent reactions in the apicoplast appear to be restricted to lipid metabolism, and the

maximal specific activity (k_{cat}) of a recently reported Fd-dependent enzyme (LytB protein) involved in isoprenoid biosynthesis in *P. falciparum* apicoplast was calculated to be as low as ~1.3/s (*13*).

The structural basis for specific recognition of PfFd by PfFNR has been analysed in the present study. Selective electron transfer from PfFNR to PfFd (Fig. 5A) may be partly explained by the differences in the redox potential. The redox potential of PfFd is −266 mV (Fig. 2), and we assume that the potential of PfFNR is similar to that of *T. gondii* FNR, estimated to be around −290 mV (*7*). These values are much more positive than those of plant counterparts (Fig. 2B), which may be one reason for the lower efficiency of electron transfer from PfFNR to plant Fds than to PfFd (Fig. 5A). Detailed analyses of molecular interaction between PfFd and PfFNR are now in progress.

Supplementary data are available at JB online.

We thank Professor Isao Taniguchi (Department of Applied Chemistry and Biochemistry, Kumamoto University, Japan) for measuring the redox potentials of Fds. This work was supported by grant in aids for Creative Scientific Research (15GSO320) and for Scientific Research on Priority Areas (13225001) from the Ministry of Education, Culture, Sports, Science and Technology of Japan.

REFERENCES

1. McFadden, G.I., Reith, M.E., Mulholland, J., and Lang-Unnasch, N. (1996) Plastid in human parasites. *Nature* **381**, 482
2. Köhler, S., Delwiche, C.F., Denny, P.W., Tilney, L.G., Webster, P., Wilson, R.J., Palmer, J.D., and Roos, D.S. (1997) A plastid of probable green algal origin in apicomplexan parasites. *Science* **275**, 1485–1489
3. Fichera, M.E. and Roos, D.S. (1997) A plastid organelle as a drug target in apicomplexan parasites. *Nature* **390**, 407–409
4. McFadden, G.I. and Roos, D.S. (1999) Apicomplexan plastids as drug targets. *Trends Microbiol.* **7**, 328–333
5. Vollmer, M., Thomsen, N., Wiek, S., and Seeber, F. (2001) Apicomplexan parasites possess distinct nuclear-encoded, but apicoplast-localized, plant-type ferredoxin-NADP$^+$ reductase and ferredoxin. *J. Biol. Chem.* **276**, 5483–5490
6. Ralph, S.A., van Dooren, G.G., Waller, R.F., Crawford, M.J., Fraunholz, M.J., Foth, B.J., Tonkin, C.J., Roos, D.S., and McFadden, G.I. (2004) Metabolic maps and functions of the *Plasmodium falciparum* apicoplast. *Nature Rev. Microbiol.* **2**, 203–216
7. Pandini, V.H., Caprini, G., Thomsen, N., Aliverti, A., Seeber, F., and Zanetti, G. (2002) Ferredoxin-NADP$^+$ reductase and ferredoxin of the protozoan parasite *Toxoplasma gondii* interact productively *in vitro* and *in vivo*. *J. Biol. Chem.* **277**, 48463–48471
8. Knaff, D.B. (1996) Ferredoxin and ferredoxin-dependent enzymes. in *Oxygenic Photosynthesis: The Light Reactions* (Ort, D.R. and Yocum, C.F., eds) pp. 333–361, Kluwer Academic Publishers, Dordrecht
9. Suzuki, A., Oaks, A., Jacquot, J.-P., Vidal, J., and Gapal, P. (1985) An electron transport system in maize roots for reaction of glutamate synthase and nitrite reductase: physiological and immunological properties of the electron carrier and pyridine nucleotide reductase. *Plant Physiol.* **78**, 374–378
10. Onda, Y., Matsumura, T., Kimata-Ariga, Y., Sakakibara, H., Sugiyama, T., and Hase, T. (2000) Differential interaction of maize root ferredoxin: NADP$^+$ oxidoreductase with photosynthetic and non-photosynthetic ferredoxin isoproteins. *Plant Physiol.* **123**, 1037–1045
11. Hanke, G.T., Kimata-Ariga, Y., Taniguchi, I., and Hase, T. (2004) A post genomic characterization of Arabidopsis ferredoxins. *Plant Physiol.* **134**, 255–264
12. Seeber, F. (2002) Biogenesis of iron-sulphur clusters in amitochondriate and apicomplexan protists. *Int. J. Parasitol.* **32**, 1207–1217
13. Rohrich, R.C., Englert, N., Troschke, K., Reichenberg, A., Hintz, M., Seeber, F., Balconi, E., Aliverti, A., Zanetti, G., Kohler, U., Pfeiffer, M., Beck, E., Jomaa, H., and Wiesner, J. (2005) Reconstitution of an apicoplast-localised electron transfer pathway involved in the isoprenoid biosynthesis of *Plasmodium falciparum*. *FEBS Lett.* **579**, 6433–6438
14. Sugiyama, T., Suzue, K., Okamoto, M., Inselburg, J., Tai, K., and Horii, T. (1996) Production of recombinant SERA proteins of *Plasmodium falciparum* in *Escherichia coli* by using synthetic genes. *Vaccine* **14**, 1069–1076
15. Sano, G., Morimatsu, K., and Horii, T. (1994) Purification and characterization of dihydrofolate reductase of *Plasmodium falciparum* expressed by a synthetic gene in *Escherichia coli*. *Mol. Biochem. Parasitol.* **63**, 265–273
16. Matsumura, T., Kimata-Ariga, Y., Sakakibara, H., Sugiyama, T., Murata, H., Takao, T., Shimonishi, Y., and Hase, T. (1999) Complementary DNA cloning and characterization of ferredoxin localized in bundle-sheath cells of maize leaves. *Plant Physiol.* **119**, 481–488
17. Taniguchi, I., Miyahara, A., Iwakiri, K., Hirakawa, Y., Hayashi, Y., Nishiyama, K., Akashi, T., and Hase, T. (1997) Electrochemical study of biological functions of particular evolutionary conserved amino acid residues using mutated molecules of maize ferredoxin. *Chem. Lett.* **1977**, 929–930
18. Pflugrath, J.W. (1999) The finer things in X-ray diffraction data collection. *Acta Cryst.* **D55**, 1718–1725
19. Brünger, A.T., Adams, P.D., Clore, G.M., DeLano, W.L., Gros, P., Grosse-Kunstleve, R.W., Jiang, J.-S., Kuszewski, J., Nilges, M., Pannu, N. S., Read, R. J., Rice, L. M., Simonson, T., and Warren, G. L. (1998) Crystallography & NMR system: a new software suite for macromolecular structure determination. *Acta Cryst.* **D54**, 905–921
20. Aoki, S., Li, J., Itagaki, S., Okech, B.A., Egwang, T.G., Matsuoka, H., Palacpac, N.M.Q., Mitamura, T., and Horii, T. (2002) Serine repeat antigen (SERA5) is predominantly expressed among the SERA multigene family of *Plasmodium falciparum*, and the acquired antibody titers correlate with serum inhibition of the parasite growth. *J. Biol. Chem.* **277**, 47533–47540
21. Takeo, S., Kokaze, A., Ng, C.S., Mizuchi, D., Watanabe, J., Tanabe, K., Kojima, S., and Kita, K. (2000) Succinate dehydrogenase in *Plasmodium falciparum* mitochondria: molecular characterization of the *SDHA* and *SDHB* genes for the catalytic subunits, the flavoprotein (Fp) and iron-sulfur (Ip) subunits. *Mol. Biochem. Parasitol.* **107**, 191–205
22. Couture, M.M., Colbert, C.L., Babini, E., Rosell, F.I., Mauk, A.G., Bolin, J.T., and Eltis, L.D. (2001) Characterization of BphF, a Rieske-type ferredoxin with a low reduction potential. *Biochemistry* **40**, 88–92
23. Striepen, B., Crawford, M.J., Shaw, M.K., Tilney, L.G., Seeber, F., and Roos, D.S. (2000) The plastid of *Toxoplasma gondii* is divided by association with the centrosomes. *J. Cell Biol.* **151**, 1423–1434
24. Bednarek, A., Wiek, S., Lingelbach, K., and Seeber, F. (2003) *Toxoplasma gondii*: Analysis of the active site insertion of its ferredoxin-NADP$^+$-reductase by peptide-specific antibodies and homology-based modeling. *Exp. Parasitol.* **103**, 68–77
25. He, C.Y., Striepen, B., Pletcher, C.H., Murray, J.M., and Roos, D.S. (2001) Targeting and processing of nuclear-encoded

apicoplast proteins in plastid segregation mutants of *Toxoplasma gondii*. *J. Biol. Chem.* **276**, 28436–28442
26. Binda, C., Coda, A., Aliverti, A., Zanetti, G., and Mattevi, A. (1998) Structure of the mutant E92K of [2Fe-2S] ferredoxin I from Spinacia oleracea at 1.7 A resolution. *Acta Crystallogr. Sect. D: Biol. Crystallogr.* **54**, 1353–1358
27. Weber-Main, A.M., Hurley, J.K., Cheng, H., Xia, B., Chae, Y.K., Markley, J.L., Martinez-Julvez, M., Gomez-Moreno, C., Satnkovich, M.T., and Tollin, G. (1998) An electrochemical, kinetic, and spectroscopic characterization of [2Fe-2S] vegetative and heterocyst ferredoxins form Anabaena 7120 with mutations in the cluster binding loop. *Arch. Biochem. Biophys.* **355**, 181–188
28. Gou, P., Hanke, G.T., Kimata-Ariga, Y., Satandley, D.M., Kubo, A., Taniguchi, I., Nakamura, H., and Hase, T. (2006) Higher order structure contributes to specific differences in redox potential and electron transfer efficiency of root and leaf ferredoxins. *Biochemistry* **45**, 14389–14396
29. Akashi, T., Matsumura, T., Ideguchi, T., Iwakiri, K., Kawakatsu, T., Taniguchi, I., and Hase, T. (1999) Comparison of the electrostatic binding sites on the surface of ferredoxin for two ferredoxin-dependent enzymes, ferredoxin-$NADP^+$-reductase and sulfite reductase. *J. Biol. Chem.* **274**, 29399–29405
30. Aliverti, A., Faber, R., Finnerty, C.M., Ferioli, C., Pandini, V., Negri, A., Karplus, P.A., and Zanetti, G. (2001) Biochemical and crystallographic characterization of ferredoxin-$NADP^+$-reductase from nonphotosynthetic tissues. *Biochemistry* **40**, 14501–14508